(4) (a) Tsuchida, E. *J. Macromol. Sci., Chem.* **1979**, *A13*, 545. (b) Tsuchida, E.; Nishide, H.; Yuasa, M.; Hasegawa, E.; Matsushita, Y.; Eshima, K. *J. Chem. Soc., Dalton Trans.* **1985**, 275. (c) Tsuchida, E. *Ann. N.Y. Acad. Sci.* **1985**, *446*, 429. (d) Tsuchida, E. *Chem. Eng. News* **1985**, *63*(2), 42.
(5) (a) Koval, C. A.; Noble, R. D.; Way, J. D.; Lovie, B.; Reyes, Z. E.; Batman, B. R.; Horn, G. M.; Reed, D. L. *Inorg. Chem.* **1985**, *24*, 1147. (b) Roman, I. C.; Baker, I. W. U.S. Patent 4 542 010, 1985.
(6) Nishide, H.; Ohyanagi, M.; Okada, O.; Tsuchida, E. *Macromolecules* **1986**, *19*, 495.
(7) (a) Nishide, H.; Kuwahara, M.; Ohyanagi, M.; Funada, Y.; Kawakami, H.; Tsuchida, E. *Chem. Lett.* **1986**, 43. (b) Drago, R. S.; Balkus, K. J. *Inorg. Chem.* **1986**, *25*, 716. (c) Nishide, H.; Ohyanagi, M.; Kawakami, H.; Tsuchida, E. *Bull. Chem. Soc. Jpn.* **1986**, *59*, 3213.
(8) Collman, J. P.; Brauman, J. I.; Coxsee, K. M.; Halbert, T. R.; Hayes, S. E.; Suslick, K. S. *J. Am. Chem. Soc.* **1978**, *100*, 2761.
(9) (a) Paul, D. R.; Koros, W. J. *J. Polym. Sci., Polym. Phys. Ed.* **1976**, *14*, 675. (b) Paul, D. R. *Ber. Bunsen-Ges. Phys. Chem.* **1979**, *83*, 294.
(10) (a) Wohrle, D.; Bohlen, H.; Aringer, C. *Makromol. Chem.* **1984**, *185*, 669. (b) Tsuchida, E.; Honda, K.; Hata, S. *Bull. Chem. Soc. Jpn.* **1976**, *49*, 868.
(11) Beugelsdijk, T.; Drago, R. S. *J. Am. Chem. Soc.* **1975**, *97*, 6466.

Relaxation Behavior of the β Phase of Poly(butylene terephthalate)

B. C. Perry, J. L. Koenig,* and J. B. Lando

Department of Macromolecular Science, Case Western Reserve University, Cleveland, Ohio 44106. *Received June 30, 1986*

ABSTRACT: Poly(butylene terephthalate) undergoes a unique reversible crystalline α to β phase transition when uniaxially drawn. The strained (β) phase of poly(butylene terephthalate) was obtained in a metastable form by cold-drawing a fiber sample approximately 250% (>50% crystallinity). Wide-angle X-ray diffraction, diffuse-reflectance IR, and ^{13}C CP-MAS-DD experiments confirm the presence of the β phase. ^{13}C relaxation measurements involving spin-lattice relaxation in the rotating frame, $T_{1\rho}$, indicate that the aromatic rings in the β phase possess more molecular motion than those in the α phase. Spin-lattice relaxation measurements, T_1, indicate that the terephthalate residue has increased mobility with respect to the α phase, which indicates the driving force behind the reversible crystal-crystal transition is indeed the packing efficiency of the aromatic rings in the α phase. The interior methylenes have motions of greater frequency and or amplitude with respect to the exterior methylenes in both phases.

Introduction

^{13}C NMR spectroscopy is an analytical tool that not only probes static structural information but also allows dynamic measurements over a broad frequency range. The available frequency range is from the kilohertz region (^{13}C $T_{1\rho}$) to the megahertz region (^{13}C T_1). The relaxation behavior of the α-crystalline phase of poly(butylene terephthalate) (PBT) (Figure 1) has been studied extensively by Jelinski et al.[1-10] The β-crystalline phase in PBT has not been studied to date by ^{13}C NMR.

PBT is a unique polymer because it undergoes a reversible crystal-crystal phase transition when uniaxially stretched. It has been clearly shown by IR and WAXS[11-26] that the α (relaxed) to β (strained) transition occurs at strains as low as 5% and that the transition is complete at 15% strain. When tension is released, the polymer reverts rapidly back to the α phase with little hysteresis. Static measurements have shown the major differences between the phases lies in the conformation of the tetramethylene segments. The α phase is A-T-A (where A = non-trans, non-gauche and T = trans) and the β phase is the extended T-T-T configuration. It is believed that the driving force behind the reversible transition is the enhanced packing efficiency of the terephthalate groups in the α phase.

In the past, constant tension was required to maintain a stable β phase. The restraint of constant tension precluded magic-angle spinning NMR experiments. This problem has been avoided by using a fiber sample obtained from Celanese Corp. The fiber, as spun, is an oriented, semicrystalline sample with the α phase being the dominant form. Cold-drawing the fibers approximately 250% and releasing the tension create an oriented "metastable" β phase for which magic-angle spinning (MAS) experiments can be performed. Infrared studies of the β-phase fibers before and after the MAS NMR experiment show negligible change in the amount of β phase.

In this paper, MAS-CP-DD experiments are reported on this "metastable" β phase. In addition, T_1 and $T_{1\rho}$ measurements are reported for both phases.

Experimental Section

A commercially prepared melt-spun semicrystalline PBT fiber sample was obtained from Celanese Corp. The unstretched fibers refer to the samples as received. Drawn fibers are obtained by cold-drawing on a stretch rack at room temperature to a strain of approximately 250%. Annealed samples are obtained by heating the fibers at 200 °C for approximately 8 h in vacuo with no tension.

Diffuse-reflectance (DRIFT) IR spectra are obtained on a FTS-20 Digilab FTIR spectrophotometer equipped with a narrow band-pass mercury cadmium telluride (MCT) detector. All spectra are recorded in the absorbance mode with double precision at a resolution of 2 cm^{-1}. Two hundred scans of both sample and KBr reference are collected to obtain a better S/N ratio. All spectra are transferred to a DEC VAX 11/780 computer operating under VMS 3.7 for data processing. The reflectance spectra are plotted according to the Kubelka-Monk algorithm.

Wide-angle X-ray diffraction patterns are obtained with a Statton camera (nickel-filtered Cu Kα radiation, λ = 1.5418 Å). Sample-to-film distance is calibrated with CaF_2 powder. The exposure time for each sample varied, depending on the degree of crystallinity and sample-to-film distance.

^{13}C NMR spectra are recorded at 37.7 MHz on a modified Nicolet NT-150 spectrometer. Magic-angle spinning,[27] cross polarization[28] and dipolar decoupling[29] are used simultaneously for the CP experiments. The radio-frequency fields are typically

0024-9297/87/2220-0422$01.50/0

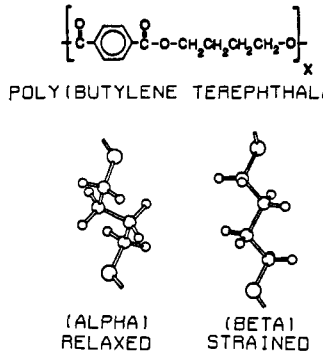

Figure 1. Repeat unit of poly(butylene terephthalate) and the conformations of the α and β phases. The α phase is A–T–A while the β phase is T–T–T (adapted from Figure 12 of ref 24).

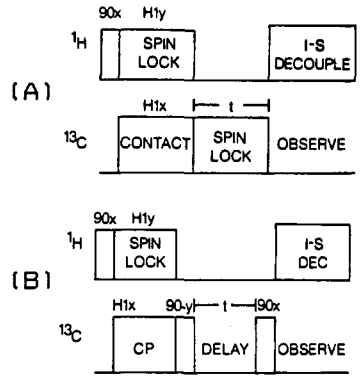

Figure 2. (A) ^{13}C $T_{1\rho}$ pulse sequence. (B) ^{13}C T_1 inversion–recovery with CP pulse sequence.

60–70 kHz. The contact time is 1 ms, with delays between successive transients of 2 s. Rotors are machined from poly(oxymethylene) (POM), and a Beams–Andrew spinning design is used. The POM resonance is used as the chemical shift reference (89.1 ppm downfield from tetramethylsilane in CP). Spinning frequencies are between 3.0 and 3.6 kHz. Samples are packed in the spinner by aligning the fibers along the rotation axis and wrapping in Teflon tape. Several thousand transients are recorded for each spectrum. The FID is collected in a 1K data size and zero-filled to 8K before Fourier transformation. The magic angle is set by maximizing the ratio of carbonyl to methylene peak using glycine. The Hartmann–Hahn match is set by maximizing peak intensities of adamantane. The 90° pulse is determined by finding the 360° and 720° pulses via nulling out of the adamantane signal. The radio-frequency field is calculated directly from the 90° pulse. The only experiments not run on the aforementioned probe are the $T_{1\rho}$ experiments run at a radio-frequency field of 46 kHz. In this case a Doty probe was utilized. Cylindrical spinners made from sapphire with Delrin caps were used. The spinning speeds were approximately 3–3.5 kHz.

^{13}C $T_{1\rho}$ experiments are performed according to the pulse sequence of Schaefer et al.[30] (Figure 2A). Delay times of 100 μs to 15 ms are used. Several thousand transients are taken for each time. CP is followed by a delay with the proton H_1 field turned off. The carbon magnetization is spin-locked to the carbon radio-frequency field so the relaxation processes are governed by kilohertz motions. Following the delay, the proton H_1 field is turned on, and the carbon signal is observed with dipolar decoupling. A semilogarithmic plot of the loss of carbon magnetization vs. delay time yields a relaxation curve with a slope that is proportional to the average ^{13}C $T_{1\rho}$ time constant.

T_1 inversion–recovery experiments using CP[31,32] were performed with the pulse sequence in Figure 2B. Delay times of 100 ms to 15 s are needed for all peaks to invert. Approximately one thousand transients are taken for each delay time.

The $T_{1\rho}$ experiments are run in sets of two so that two separate measurements are obtained and compared. The relaxation times reported are an average of a number of separate experiments. The experimental delay times are interwoven randomly so that biasing problems can be avoided.

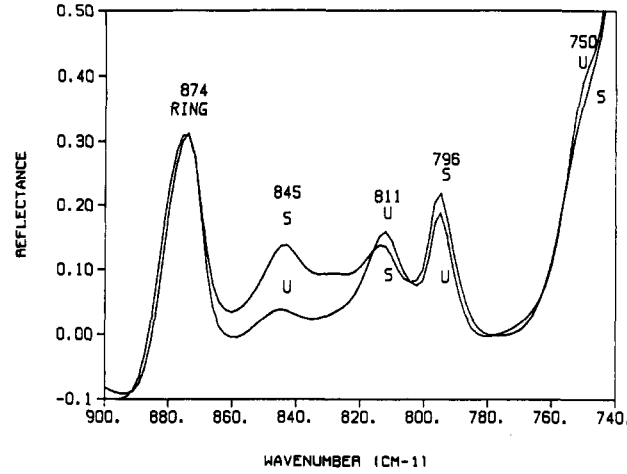

Figure 3. Comparison of the 740–900-cm^{-1} region of the drawn and undrawn fiber samples of PBT (>50% crystallinity) obtained with DRIFT.

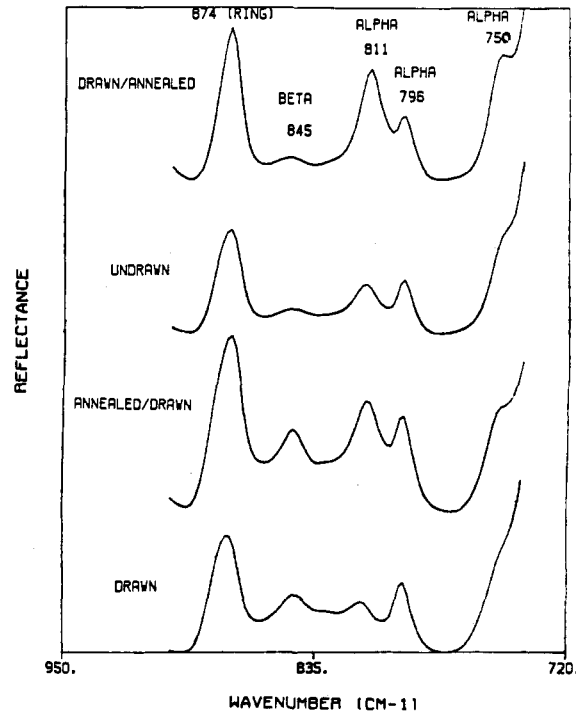

Figure 4. Comparison of the 740–900-cm^{-1} region of the drawn/annealed undrawn, annealed/drawn, and drawn fiber samples of PBT (>50% crystallinity) obtained with DRIFT after 1 day of magic-angle spinning.

Results

Diffuse-reflectance spectroscopy (DRIFT) was chosen as the IR technique to study the fibers because of the ease of sample preparation. Past IR data have shown the 740–900-cm^{-1} region to be sensitive to applied stress.[11-26] The 740–900-cm^{-1} region is less sensitive to the phase change in transmission with respect to the 900–1000-cm^{-1} region but it is more sensitive when DRIFT is used because weaker bands tend to be enhanced with this technique. The 740–900-cm^{-1} region is dominated by five peaks (Figures 3 and 4). Three of the peaks, 811, 796, and 750 cm^{-1}, are sensitive to the α phase, while the 845-cm^{-1} peak is sensitive to the β phase. The 874-cm^{-1} C–C ring mode is not altered appreciably[13] with stress; thus this peak is used to scale the absorbances of the various spectra. Figure 3 shows the characteristic changes that occur when the fibers are drawn. DRIFT spectra recorded after approximately 1 day of magic-angle spinning showed that the

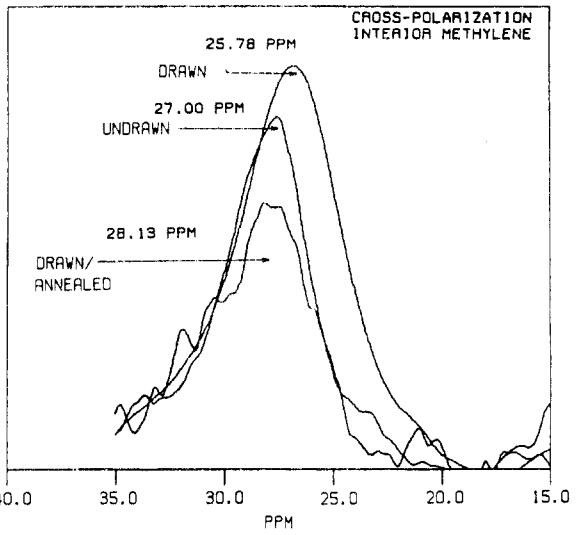

Figure 5. Overlay of the interior methylene region of the drawn, drawn/annealed, and undrawn fiber samples obtained with CP-MAS-DD (>50% crystallinity).

Table I
Chemical Shift (ppm) Values Relative to Me_4Si for Various PBT Fiber Samples Obtained with the Cross-Polarization Pulse Sequence[a]

	C=O	NPAR	PAR	OCH_2	CB_2
annealed drawn	165.7	134.8	130.6	67.0	26.1
drawn annealed	166.1	135.6	131.7	66.2	28.1
undrawn	166.2	135.8	131.4	66.0	27.0
drawn	166.1	135.2	131.0	66.3	25.8

[a] Measurements made at 20 °C.

Table II
^{13}C $T_{1\rho}$ Values (ms) for the Unstretched (α) and Stretched (β) PBT Fibers

	60–66 kHz		46 kHz	
	α	β	α	β
PAR	9.3[a,b]	6.2	6.0	3.4
OCH_2	6.0	5.0	4.6	2.9
CH_2	5.6	5.6	3.8	3.7

[a] Measurements are within 15% experimental error. [b] Measurements are made at 20 °C.

force from rapid rotation does not relax the β phase (Figure 4).

Wide-angle X-ray diffraction and electron diffraction are also used to characterize the fibers for a variety of sample preparations.[33-40] There are some characteristic changes that occur when the polymer is drawn.[34-37] The as-spun X-ray fiber pattern is characteristic of the α phase, and the drawn fiber pattern is indicative of the β phase.

The CP spectra of the samples are quite similar except for the ppm shifts of the interior methylene carbons. An overlay of the interior methylene peaks for the unstretched (α), stretched (β), and drawn/annealed (α) samples is shown in Figure 5. As the amount of trans content (β) increases, the interior methylene peak shifts to a higher field. The ppm shifts are listed in Table I.

A typical ^{13}C $T_{1\rho}$ curve obtained for the protonated carbons of PBT is shown in Figure 6. As is observed with most polymers, the curve is not linear due to multiple relaxation times. The $T_{1\rho}$ values are calculated from the initial slopes from 200 to 1000 μs. Points before 200 μs are not used to avoid transient oscillations.[30] The $T_{1\rho}$ values obtained for the unstretched (α) and stretched (β) samples are listed in Table II. The samples were used based on the relatively low levels of crystallinity. Annealed

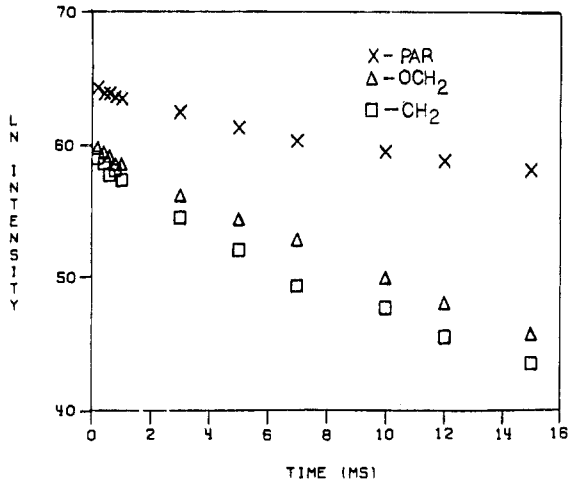

Figure 6. $T_{1\rho}$ relaxation curve of the protonated carbons of PBT (>50% crystallinity) in the β phase.

Table III
^{13}C T_1 Values (s) Obtained from the T_1 Inversion-Recovery Experiment

	unstretched (α)	stretched (β)
C=O	17.0[a,b,d]	15.0
NPAR	20.0	16.0
PAR(C)	9.8	7.3
PAR(A)	5.0[c]	4.3
OCH_2	0.39	0.44
CH_2	0.22	0.23

[a] Measurements are within 15% experimental error. [b] T_1 values obtained from null points for the C=O, NPAR, and PAR(C) carbons. [c] T_1 values obtained from curve fitting for the PAR(A), OCH_2, and CH_2 carbons. [d] Measurements are obtained at 20 °C.

samples with higher levels of crystallinity are avoided due to the possible overriding effect of spin–spin diffusion in highly coupled protonated polymers.

A major problem in interpreting $T_{1\rho}$ values is the possibility that spin–spin diffusion contributes to the relaxation. Schaefer et al.[41] have outlined a detailed nine-step procedure in which relative amounts of spin–spin and spin–lattice contributions can be obtained. A more qualitative determination can be made from the carbon H_1 field dependence. A $T_{1\rho}$ value dominated by spin–spin diffusion should vary by a factor of 10 for each increase in H_1(C) equal to half the proton line width,[42] which is on the order of 20 kHz. Measurements were made at a carbon radio-frequency field of 46 kHz and 60–66 kHz, and the values obtained are listed in Table II. The relative error for all measurements is ±15%. The increase in the $T_{1\rho}$ values for the higher H_1(C) field is small, indicating a predominantly motional basis for the $T_{1\rho}$.

The T_1 values were obtained by fitting the relaxation to the inversion–recovery equation. This is done by using a program provided by Dr. Skarjune of 3M called RELAX. The curve fitting is done for the aliphatic carbons and the faster relaxing protonated aromatic carbon (PAR) peak. The slower relaxing peaks, which include the nonprotonated carbons and a slower relaxing component of the PAR peak, were not analyzed as they did not show adequate recovery due to the long times required for inversion to occur. The T_1 values for these carbons were estimated from the null points. The experimental values are listed in Table III for the unstretched, stretched, and drawn/annealed fiber samples. The reported values for the unstretched and stretched samples are an average of 3–5 measurements, while the drawn/annealed value is one measurement. The error in the measurements is ±15%.

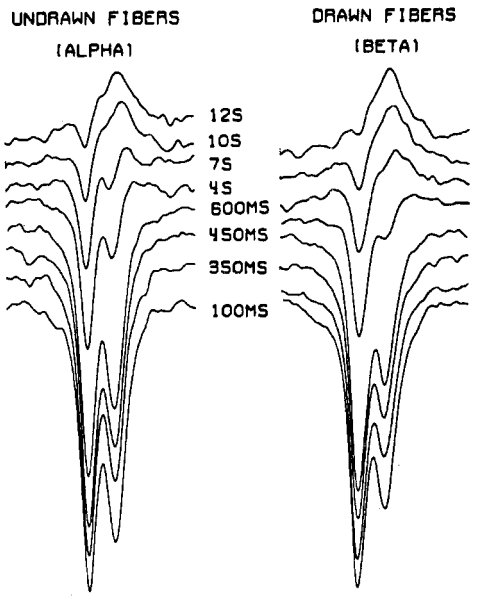

Figure 7. Expanded view of the relaxation behavior of the aromatic peaks of the drawn and undrawn PBT fibers using T_1 inversion–recovery (>50% crystallinity).

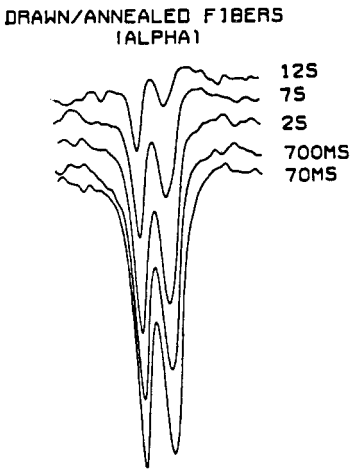

Figure 8. Expanded view of the relaxation behavior of the aromatic peaks of the drawn/annealed PBT fibers using T_1 inversion–recovery (>50% crystallinity).

The terephthalate carbons in the β phase relax more efficiently than the α-phase counterparts. The relaxation times of the aliphatic carbons of the β phase and α phase are identical. The T_1 values of the drawn/annealed fiber sample indicate that the terephthalate groups relax much slower than either the drawn or as-spun samples. The methylenes are affected to a much lesser extent, with the exterior methylenes relaxing identically and the interior methylenes slowing. Figures 7 and 8 are expanded regions of the PAR inversion–recovery for the various samples, and it is clear that the relaxation time differences are supported by visual observation of the null point.

Discussion

The ability to discern between the α and β phases using IR is well-known.[11-26] In particular, the 740–900-cm^{-1} region (Figures 3 and 4) is the most sensitive to the phase change changes with DRiFT. The cold-drawn or stretched fibers have an increase in the peaks sensitive to the β phase. The β band at 845 cm^{-1} increases upon drawing. The bands sensitive to the α-phase tetramethylene configuration decrease upon stretching, indicating that significant α to β conversion has taken place. The amorphous

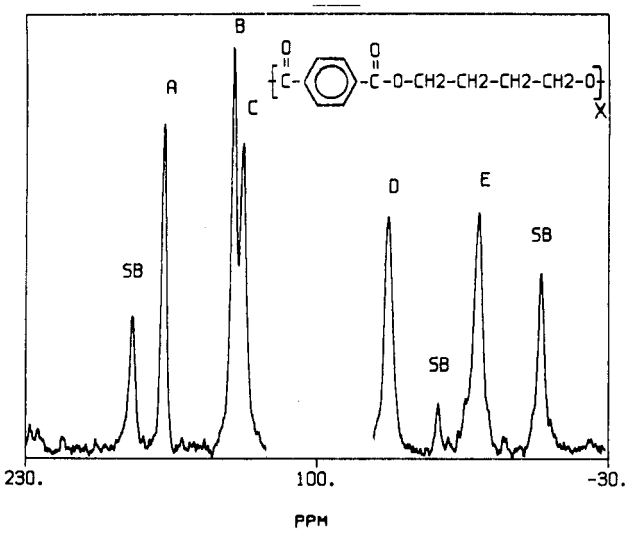

Figure 9. Cross polarization–magic-angle spinning–dipolar decoupling spectrum of the stretched (β) PBT fibers (>50% crystallinity).

regions of the polymer contain some A–T–A tetramethylene configurations that contribute to the α absorbances. The drawn polymer is not held under tension; thus the IR measurements indicate that a relatively stable β phase is obtained when the polymer is drawn at room temperature. The polymer does relax back to the α phase over a period of several days. In addition, Figure 4 indicates that forces generated by magic-angle spinning do not appreciably alter the phase of the cold-drawn fibers.

X-ray diffraction confirmed the infrared results. Past work has shown significant changes in the X-ray pattern occur upon conversion from the α to β phases.[34-37] The intense $1\bar{1}1$ reflections in the α phase are absent in the β phase. The $\bar{1}11$ and 011 reflections that are on the first layer line but close to the equator in the α phase merge into one reflection in the β phase. There is also a characteristic lengthening of the *c*-axis repeat in the β phase, which is observed as the $0\bar{1}4$ reflection moves closer to the center beamstop. The unstretched fibers are semicrystalline, oriented, and exist in the α phase. Drawing the fibers induces some crystallization as less amorphous background is observed. The diffraction pattern confirms that the drawn sample exists in the β phase.

Cross-polarization utilizes MAS–CP–DD to obtain a spectrum. The spinning removes chemical shift anisotropy, and the dipolar decoupling removes the static interaction between the carbon and hydrogen nuclei. CP utilizes the higher polarization and the shorter T_1 values of the protons to enhance the sensitivity of the carbon spectra. The crystalline and amorphous phase carbons are sensitive to the CP pulse sequence.

A characteristic PBT ^{13}C CP–MAS–DD spectrum of the β phase appears in Figure 9. There are five peaks: the carbonyl (C=O), nonprotonated aromatic (NPAR), protonated aromatic (PAR), exterior methylenes (OCH_2), and interior methylenes (CH_2). The ppm values are listed in Table I. A comparison of chemical shift values indicates that the interior methylene carbon is the only one that has a major shift (Figure 5). The CH_2 carbon for the drawn fiber appears at 25.8 ppm, the undrawn fiber is at 27.0 ppm, and the drawn/annealed fiber CH_2 appears at 28.1 ppm. The shifts agree quite well with model compound work done by Havens and Koenig,[43] which showed that as more trans content is introduced, the peak shifts to a higher field. The ppm shift of the undrawn CH_2 is between the drawn and drawn/annealed due to β conformation

being present in the amorphous regions.

The shift of the CH_2 carbons confirms past data that have indicated that the main difference between the two phases lies in the conformation of the tetramethylene segment. The shift is most likely due to the spatial effects of the oxygen atom relative to the interior methylene carbons in the crumpled form, thus shielding the CH_2 carbon to a greater extent.

Dynamic NMR Measurements

^{13}C $T_{1\rho}$ measurements probe motional dynamics in the kilohertz region and have been correlated with mechanical properties by Schaefer et al.[44-47] Jelinski et al. have shown that the motion of the aromatic rings for the relaxed phase is reflected in CSA and deuterium-labeling experiments.[1,5] The aliphatic carbons were found to be more sensitive to T_1 measurements.[2-4]

A comparison of the $T_{1\rho}$ values of both the stretched and unstretched samples at the different radio-frequency fields indicates that the $T_{1\rho}$ values vary in a range between linearly with the field and the square of the field. More radio-frequency field values are needed in order to precisely determine the order of the variance. The approximate square field dependence of the relaxation times means that there are significant contributions from motions below the carbon radio-frequency field.[47] If significant motional contributions occurred only at much faster correlation times, then very little field dependence would be expected.

Spin–spin diffusion is often a problem when semicrystalline polymers are studied. Jelinski et al.[3] have shown that $T_{1\rho}$ measurements on PBT were mainly spin–lattice in character. The relatively small radio-frequency field dependence does indeed confirm the spin–lattice contribution to the $T_{1\rho}$ values.

A typical $T_{1\rho}$ curve has a minimum in its relaxation time vs. correlation time plot. The slow side of the curve can be interpreted in such a way that a decrease in a $T_{1\rho}$ value indicates increased molecular motion.

A qualitative approach is to observe the effect of varying the radio-frequency field. The fact that the $T_{1\rho}$ value does change indicates that the time constant lies on the slow side of the minimum. A high-side relaxation time would be rather insensitive to the radio-frequency field.

A comparison of the interior and exterior methylene carbons within the α and β phases indicates no difference between the carbons. However, the exterior methylene carbons of the β phase possess more mobility than their counterparts in the α phase as the $T_{1\rho}$ value is shorter at both radio-frequency field strengths. The interior methylene carbons show no significant differences. The PAR carbons, which are known to undergo ring flips and rapid librational motions, do indeed differ. The value in the α phase is 9.3 ± 1.4 ms while its counterpart in the β phase is 6.2 ± 1.0 ms. The relative difference is observed at 46 kHz, with the relaxed phase being 6.0 ± 1.0 ms and the strained form being 3.4 ± 0.5 ms.

The differences can be interpreted in terms of the β-phase rings possessing more molecular freedom than those in the α phase. The β-phase unit cell has a larger volume than the α phase. In this case, there are smaller intermolecular and intramolecular forces so the rings are more mobile. The packing in the α phase is thought to be more efficient. Better packing is synonymous with less motion. Orientation due to drawing would tend to slow down carbons as a result of inducing better packing of the repeat units; thus longer $T_{1\rho}$ values would be expected if this were the only change. X-ray diffraction photographs of the β phase indicate that the 100 equatorial reflection is blurred, which can be interpreted as poorer packing. The driving force behind the reversible transition is thought to be the improved packing efficiency of the phenyl rings in the α phase.

^{13}C spin–lattice T_1 measurements were also performed in order to correlate trends seen in the ^{13}C $T_{1\rho}$ experiments. Past work by Jelinski et al.[2-4] on the relaxed form showed that the aliphatic carbons are sensitive to the T_1 measurement. The heterogeneity of the ring motions should also make the PAR carbon sensitive to megahertz motions.

The interpretation of T_1 relaxation times is somewhat easier than $T_{1\rho}$ relaxation times because contributions from spin–spin interactions are considered insignificant.[48] Protonated carbons will be the most sensitive to the measurement because CP is used to build up the carbon signal. Past work[3] has shown the PBT carbons to lie on the slow motion side of the T_1 minimum.

Jelinski et al.[3] measured T_1 values for the α phase of PBT, and the results were 2 s for the PAR carbons, 0.47 s for OCH_2, and 0.3 s for CH_2. The smaller T_1 for the interior methylene carbons agreed with CSA measurements[1] and deuterium-labeling experiments[4] which indicated that the interior methylene carbons were undergoing motions of higher frequency and/or larger amplitude than the exterior methylenes. Helfand-type motions[49] were postulated, particularly the four-carbon type motions of the aliphatic segment with the terephthalate groups acting as molecular anchors.

The T_1 measurements obtained in this study on the unstretched fibers (α) are listed in Table III. The aliphatic carbon values of 0.39 ± 0.05 s for OCH_2 and 0.22 ± 0.03 for CH_2 agree quite well with Jelinski's measurements. A minor discrepancy exists between the PAR carbon values, as a value of 5 ± 0.5 s is obtained in this study compared to Jelinski's value of 2 s. The T_1 values for the stretched (β) fibers are listed in Table III. A similar trend is observed for the aliphatic carbons, with the OCH_2 value of 0.44 ± 0.05 s and the CH_2 value of 0.23 ± 0.04. The time constants are identical within experimental error to the α-phase aliphatics, which suggests that the high-frequency motions of the aliphatic carbons are nearly the same for both trans and non-trans, non-gauche conformations.

In order to compare the two phases, one must make the assumption that the β-phase T_1 values lie on the slow side of the T_1 minimum. The aliphatic carbons show no significant motional changes. A comparison of the $T_{1's}$ for the terephthalate carbons, and, in particular, the PAR carbons, shows that the β-phase aromatic rings possess more molecular mobility. The same trend is observed with $T_{1\rho}$ measurements, which infers that the ring motions are very heterogeneous. A decrease in the NPAR T_1 indicates that there is significant in-plane motion in the β phase.

An inversion–recovery experiment was also performed on a drawn/annealed sample. The sample is a highly crystalline oriented α phase. Inspection of Figure 8 clearly shows that at 12 s all the terephthalate carbons are negative, whereas the carbon peaks for the stretched and unstretched samples (Figure 7) are all positive by 12 s. The aliphatic carbons are slightly lengthened by the above process but the affect is rather small. It is an indication that the terephthalate carbons are slowed considerably by packing in the crystalline regions of the α phase.

An expanded view of the aromatic region of the CP spectrum for the unstretched fibers shows the PAR peak to have a shoulder at 131.7 ppm. The D/A CP spectrum has its main aromatic peak at 131.7 ppm, which indicates that this is a crystalline aromatic contribution. The T_1 inversion–recovery experiments also show a splitting of the

protonated aromatic peak. There is a broad component that inverts at approximately 4–5 s and is located at 129 ppm and is the value in Table III obtained from curve fitting. There is also a smaller sharper peak at 133 ppm that takes much longer to invert. This is attributed to the crystalline aromatic carbons. Curve fitting was not done because there was very little recovery. As a result null point estimates are reported. It is apparent that the broad PAR peak is slightly slower in the α phase, while the sharper peak is much slower to invert. This is an indication that the packing of the rings in the crystalline regions of the α phase is much preferred because the molecular mobility is reduced.

The use of static IR and X-ray measurements as well as simple ^{13}C NMR experiments has shown that a "metastable" β phase can be obtained. The differences between the α and β phases are relatively small, and these appear as intensity shifts in IR spectra, ppm shifts in NMR spectra, and the disappearance of peaks in X-ray patterns. Dynamic NMR measurements probing both the kilohertz and megahertz frequency ranges indicate that the terephthalate groups have more molecular freedom in the β phase. At the higher frequencies the OCH_2 and CH_2 carbons have very different relaxation times in both the α and β phases. In both cases, the OCH_2 carbons relax slower than the CH_2 carbons. The T_1 experiment also separates the PAR peak into two components, with the slower relaxing peak being shorter in the β phase.

Acknowledgment. We gratefully acknowledge Celanese Corp. for supplying the PBT fiber sample and NSF-MRL at Case Western Reserve University for providing graduate fellowship and research support under Grant DMR-8119425.

Registry No. PBT (SRU), 24968-12-5; PBT(copolymer), 26062-94-2.

References and Notes

(1) Jelinski, L. W. *Macromolecules* **1981**, *14*, 1341.
(2) Jelinski, L. W.; Dumais, J. J. *Macromolecules* **1983**, *16*, 403.
(3) Jelinski, L. W.; Dumais, J. J.; Watnick, P. I.; Engel, A. K.; Sefcik, M. D. *Macromolecules* **1983**, *16*, 409.
(4) Jelinski, L. W.; Dumais, J. J.; Engel, A. K. *Macromolecules* **1983**, *16*, 492.
(5) Cholli, A. L.; Dumais, J. J.; Engel, A. K.; Jelinski, L. W. *Macromolecules* **1984**, *17*, 2399.
(6) Jelinski, L. W.; Schilling, F. C.; Bovey, F. A. *Macromolecules* **1981**, *14*, 581.
(7) Jelinski, L. W.; Dumais, J. J.; Engel, A. K. *ACS Symp. Ser.* **1984**, *No. 247*, 55.
(8) Jelinski, L. W.; Dumais, J. J. *Polym. Prepr. (Am. Chem. Soc., Div. Polym. Chem.)* **1981**, *22*, 273.
(9) Jelinski, L. W.; Dumais, J. J.; Engel, A. K. 185th National Meeting of the American Chemical Society, Seattle, WA, Mar 20–25, 1983.
(10) Bovey, F. A.; Jelinski, L. W. *J. Phys. Chem.* **1985**, *89*, 571.
(11) Jakeways, R.; Ward, I. M.; Wilding, M. A.; Hall, I. H.; Desborough, I. J.; Pass, M. G. *J. Polym. Sci., Polym. Phys. Ed.* **1975**, *13*, 799.
(12) Brereton, M. G.; Davies, G. R.; Jakeways, R.; Smith, T.; Ward, I. M. *Polymer* **1978**, *19*, 17.
(13) Stambaugh, B.; Lando, J. B.; Koenig, J. L. *J. Polym. Sci., Polym. Phys. Ed.* **1979**, *17*, 1063.
(14) Stach, W.; Holland-Moritz, K. *J. Mol. Struct.* **1980**, *60*, 49.
(15) Siesler, H. W. *J. Polym. Sci., Polym. Lett. Ed.* **1979**, *17*, 453.
(16) Siesler, H. W. *Makromol. Chem.* **1979**, *180*, 2261.
(17) Siesler, H. W. *Polym. Bull. (Berlin)* **1981**, *4*, 165.
(18) Gillette, P. C. Ph.D. Thesis, Case Western Reserve University, 1983.
(19) Molis, S. E.; MacKnight, W. J.; Hsu, S. L. *Appl. Spectrosc.* **1984**, *38*, 529.
(20) Stambaugh, B. D.; Koenig, J. L.; Lando, J. B. *J. Polym. Sci., Polym. Lett. Ed.* **1977**, *15*, 299.
(21) Siesler, H. W. *Polym. Prepr. (Am. Chem. Soc., Div. Polym. Chem.)* **1980**, *21*, 163.
(22) Holland-Moritz, K.; Stach, W.; Holland-Moritz, I. *Prog. Colloid Polym. Sci.* **1980**, *67*, 161.
(23) Stach, W. Doktor Dissertation, Institut für Physikalische Chemie, Universität Koeln, Koeln, West Germany.
(24) Siesler, H. W. *J. Mol. Struct.* **1980**, *59*, 15.
(25) Stokr, J.; Schneider, B.; Doskocilova, D.; Loevy, J.; Sedlacek, P. *Polymer* **1982**, *23*, 714.
(26) Stach, W. W.; Holland-Mortiz, K. *IUPAC Proc. 28th Macromol. Symp. 1982 (Amherst, Mass.)*
(27) Andrew, E. R. *Prog. Nucl. Magn. Reson. Spectrosc.* **1972**, *8*, 1.
(28) Pines, A.; Gibby, M. F.; Waugh, J. S. *J. Chem. Phys.* **1972**, *56*, 1776.
(29) Schaefer, J. *Topics in Carbon-13 NMR Spectroscopy*; Levy, G. L., Ed.; Wiley: New York, 1974; p 149.
(30) Schaefer, J.; Stejskal, E. O.; Buchdahl, R. *Macromolecules* **1977**, *10*, 384.
(31) Sullivan, M. J.; Maciel, G. E. *Anal. Chem.* **1982**, *54*, 1606.
(32) Sullivan, M. J.; Maciel, G. E. *Anal. Chem.* **1982**, *54*, 1615.
(33) Mencik, Z. *J. Polym. Sci.* **1975**, *13*, 2173.
(34) Yokouchi, M.; Shakakibara, Y.; Chatoni, Y.; Tadakoro, H.; Tanaka, T.; Yoda, K. *Macromolecules* **1976**, *9*, 266.
(35) Hall, I. H.; Pass, M. G. *Polymer* **1976**, *17*, 807.
(36) Desborough, I. J.; Hall, I. H. *Polymer* **1977**, *18*, 825.
(37) Stambaugh, B. D.; Koenig, J. L.; Lando, J. B. *J. Polym. Sci., Polym. Phys. Ed.* **1976**, *17*, 807.
(38) Alter, U.; Bonart, R. *Colloid Polym. Sci.* **1976**, *254*, 348.
(39) Joly, A. M.; Nemoz, G.; Georges Vallet, A. D. *Makromol. Chem.* **1975**, *176*, 479.
(40) Roche, E. J.; Stein, R. S.; Thomas, E. L. *J. Polym. Sci., Polym. Phys. Ed.* **1980**, *18*, 1145.
(41) Schaefer, J.; Sefcik, M. D.; Stejskal, E. O.; McKay, R. A. *Macromolecules* **1984**, *17*, 1117.
(42) Schaefer, J.; Stejskal, E. O.; Steger, T. R.; Sefcik, M. D.; McKay, R. A. *Macromolecules* **1980**, *13*, 1121.
(43) Havens, J. R.; Koenig, J. L. *Polym. Commun.* **1983**, *24*, 196.
(44) Steger, T. R.; Schaefer, J.; Stejskal, E. O.; McKay, R. A. *Macromolecules* **1980**, *13*, 1127.
(45) Sefcik, M. D.; Stejskal, E. O.; McKay, R. A. *Macromolecules* **1980**, *13*, 1137.
(46) Schaefer, J.; Sefcik, M. D.; Stejskal, E. O.; McKay, R. A. *Macromolecules* **1984**, *17*, 1107.
(47) Sefcik, M. D.; Schaefer, J.; Stejskal, E. O.; McKay, R. A. *Macromolecules* **1980**, *13*, 1132.
(48) Levy, G. C.; Lichter, R. L.; Nelson, G. L. *Carbon-13 Nuclear Magnetic Resonance Spectroscopy*, 2nd ed.; Wiley: New York, 1980; p 191.
(49) Helfand, E. J. *J. Phys. Chem.* **1971**, *54*, 4651.